Infrared Spectroscopy of Resonantly Ionized (Phenol)$(H_2O)_n^+$

K. Kleinermanns,* Ch. Janzen, D. Spangenberg, and M. Gerhards*

Institut für Physikalische Chemie und Elektrochemie I, Heinrich-Heine-Universität Düsseldorf, D-40225 Düsseldorf, Germany

Received: November 19, 1998; In Final Form: April 21, 1999

The infrared spectra of (phenol)$(H_2O)_n^+$ cluster ions ($n = 1-4$, 7, 8) have been recorded in the region from 2850 to 3800 cm^{-1}. The method developed for this study (IR-PARI = infrared photodissociation after resonant ionization) allows sensitive IR spectroscopy of cluster ions from size-selected neutral precursors. The three-color laser scheme used for ion selection and dissociation consists of a two-color $S_0 \rightarrow S_1 \rightarrow D_0$ ionization of a mass-selected cluster followed by IR photodissociation of the cluster ion. The IR spectra were taken by monitoring the photodissociation dip of the parent ion signal and by recording the rise of the $-H_2O$ fragment signal. The experimentally observed frequencies are compared to the results of ab initio calculations. No proton transfer is observed for the (phenol)$(H_2O)_{1,2}^+$ clusters. In contrast to the S_0 state, the structure of (phenol)$(H_2O)_2^+$ turns out to be linear. In the case of the (phenol)$(H_2O)_{3,4}^+$ clusters, linear and solvated structures are discussed. Within the solvated structures, proton transfer can occur between phenol and the water molecule, which is hydrogen-bonded to phenol. The observed fragmentation thresholds indicate proton transfer for (phenol)$(H_2O)_{n\geq 4}^+$ on the nanosecond time scale of our experiment. At least for the (phenol)$(H_2O)_8^+$ cluster, the second solvation shell is full and a third solvation shell will be formed.

(I) Introduction

Hydrated organic and inorganic ions and especially the hydrated hydronium ions $(H_2O)_n \cdot H_3O^+$ are important research objects in chemistry. The solvated proton occupies a key position in the liquid-phase chemistry of aqueous solutions.[1] Microscopic studies of the proton-transfer process in the gas[2−5] and liquid phases[6] are active research topics. Small gaseous ions such as H_3O^+ and $H_5O_2^+$ were identified in the D region of the ionosphere,[7] and $(H_2O)_n \cdot H_3O^+$ ions are probably the dominant ions in this region.[8] Lee and co-workers pioneered the jet spectroscopy of $(H_2O)_n \cdot H_3O^+$ ($n = 1-8$) in the infrared spectral region of the OH stretching vibration.[3−5] The clusters were mass-selected and then trapped in a radio-frequency ion trap. H_2O evaporation was performed by OH stretching vibrational excitation and cw CO_2 laser multiphoton dissociation of these vibrationally excited species. Alternatively, IR spectroscopy was performed by excitation of OH or H_2 stretches followed by loss of H_2 in $(H_2O)_n \cdot H_3O^+ \cdot H_2$ clusters. Several symmetric and antisymmetric stretching vibrations of H_3O^+ and H_2O could be identified. Comparison of the experimentally observed frequencies with harmonic frequencies obtained from ab initio[9] and DFT[10] calculations supports the generally accepted model[1] that H_3O^+ is solvated by three water molecules in the first solvation shell. The H_2 "messenger"[4] allows single IR photon predissociation of $(H_2O)_{1-3} \cdot H_3O^+$ ions. The cluster formed by H_2 to H_3O^+ lowers the symmetry of pure H_3O^+. This leads to a splitting of the degenerate antisymmetric stretching vibrations in H_3O^+. In $H_5O_2^+ \cdot H_2$, vibrations of H_3O^+ can be observed, indicating that the $H_2O \cdot\cdot H^+ \cdot\cdot H_2O$ arrangement is no longer symmetric compared to pure $H_5O_2^+$ (ref 5). (Phenol)$(H_2O)_n^+$ can be expected to form similar structures to the hydrated hydronium ions if proton transfer takes place from (phenol)$^+$ to H_2O. The resulting phenoxy radical has a similar proton affinity as H_2O.[11]

The vibrational spectra of (phenol)$(H_2O)_{1-3,\geq 4}^+$ were measured by Sawamura et al. in the range from 3100 to 3800 cm^{-1}.[12] In their experiments, the phenol monomer was resonantly ionized in the beginning of the jet expansion. (Phenol)$^+$ reacts with some admixed water in the jet. The phenol−water cluster ions cool via collisions in the course of the expansion, get trapped in a radio-frequency ion trap, and are photodissociated in the ion trap with a pulsed tunable IR laser via multiphoton absorption. The $-H_2O$ fragments are ejected from the ion trap and are mass-analyzed. Due to the low collection efficiency obtained for larger clusters, they were not able to discriminate the IR spectra for (phenol)$(H_2O)_{n\geq 4}^+$. The electronic spectra of the phenol or phenoxy part of the cluster ions were obtained via predissociation in the visible spectral range.[11]

We compare the results of Sawamura et al. with our results and extend the measurements to larger phenol−water clusters. To perform these measurements, we introduce a different technique (IR-PARI = infrared photodissociation after resonant ionization). Using this technique, the clusters are ionized by one- or two-color, two-photon excitation via the intermediate S_1 state. The excited ions are photodissociated by pumping the OH stretching vibrations approximately 40 ns after the two UV lasers have been fired. Both the dip of the parent ion signal and the rise of the $-H_2O$ fragment signal are monitored as a function of the IR laser frequency. The high sensitivity of the technique and the good mass resolution of our time-of-flight mass spectrometer allow the study of larger cluster ions up to eight H_2O ligands. The intermediate S_1 resonance allows the study of ion formation from different neutral isomer precursors. In the case of phenol/water clusters, the neutral initial structures are of no interest due to the large structural changes between the neutrals and the ions.

* Corresponding authors. E-mails: kleinermanns@uni-duesseldorf.de; gerhards@uni-duesseldorf.de.

10.1021/jp9844819 CCC: $18.00
Published on Web 06/19/1999

(II) Experimental Method and Setup

The resonant two-photon ionization (R2PI) spectra and the IR photodissoziation spectra were measured using a vacuum apparatus with a time-of-flight (TOF) mass spectrometer and a pulsed nozzle as described elsewhere.[13] To excite the different clusters from the S_0 to the S_1 state, a frequency-doubled dye laser (LAS, LDL205) operated with Fluorescein 27 (<100−500 mJ/pulse) and pumped by the second harmonic (532 nm) of a Nd:YAG laser (Spectra Physics, GCR 170) was used. Part of the 355-nm third harmonic output (10−20 mJ/pulse) at 355 nm of the same Nd:YAG laser was used as the second color for the ionization process. For the ionization (IP) and fragmentation (FP) potential measurements of different clusters, we used an excimer (EM102, 110 mJ/pulse) pumped dye laser (Lambda Physik, ≤ 1 mJ/pulse) operated with DMQ, QUI, *p*-terphenyl, Rhodamin B, or Coumarin 153. Using Rhodamin B or Coumarin 153, the output of the dye laser was frequency-doubled. The IR photodissociation spectra of the phenol−water clusters were measured using IR light (1.5−2.5 mJ/pulse, 2850−3800 cm^{-1}), generated by difference frequency mixing of the fundamental 1064 nm (40−50 mJ/pulse) of a seeded Nd:YAG laser (Spectra Physics GCR 3) and the output (15−20 mJ/pulse, 758−816 nm) of a dye laser (LAS) pumped by the frequency-doubled output of the same Nd:YAG laser. For the dye laser, a 1:1 mixture of Styryl 8 and Styryl 9 was used.

The time delay between the two UV lasers and the IR laser was controlled by a DG 535 clock (Stanford research). Measuring the photodissociation spectra, the IR laser pulse was fired 40 ns after the UV laser pulses. Small clusters ($n \leq 3$) have been ionized via one-color excitation; the larger clusters ($n = 3-8$) are ionized via two-color excitation.

For clusters $n > 1$, we observed a very slow and strongly nonlinear change of the ion signals close to the IP or the FP. Thus, linear interpolation to a defined threshold is impossible. The following statistical procedure has been used to determine the threshold energies: First, the linear baseline region on the lower (red) side of the threshold energy was determined and fitted by linear least squares to calculate the random noise standard deviation, which is needed in the statistical test later. After baseline subtraction, the data were smoothed to reduce the effect of outliers by use of a 35-, 75-, 101-, or 201-point binomial filter, which is known to have excellent filter properties.[14] The upper and lower limits of the threshold were determined by the two-sided 95% and 5% Student *t* mean difference thresholds between baseline zero and the smoothed data values. It is assumed that the true threshold energy is equally distributed inside the region between these limits with standard deviation $D/\sqrt{12}$. In the following we define the excess energy necessary for fragmentation as the difference between the fragmentation potential and the ionization potential (FP − IP).

Due to an electrical field (F) of about 83 V/cm, which accelerates the ions into the second acceleration region of the TOF, the IP data have to be corrected by $cF^{1/2}$. A series of IP measurements of the $n = 1$ cluster were performed at different electrical field strengths to determine the factor c. According to these measurements, we obtained a factor $c = 6.40 \pm 0.29$ $V^{-1/2}$ $cm^{-1/2}$ and IP_0 of 64 019 ± 4 cm^{-1}. Factor c is very close to the theoretical value of about 6 $V^{-1/2}$ $cm^{-1/2}$ for adiabatic ionization,[15] and the resulting IP deviates only by 5 cm^{-1} from the experimental $IP_0 = 64\,024.5 \pm 5$ cm^{-1} obtained from ZEKE spectra.[16] Thus, all ionization and fragmentation thresholds were corrected by $c(83^{1/2})$ V/cm = +58 cm^{-1}.

Phenol (p.a., Riedel-de Haën) was used without further purification. The temperature of the water reservoir was held at −5 to +5 °C (depending on the cluster size). Helium (2 bar) was used as the carrier gas.

(III) Theoretical Results

Re and Osamura[17] published UHF, UMP2, and DFT (B3LYP functional) calculations on $(phenol)(H_2O)_{1-3}^+$ as well as UHF and DFT calculations on $(phenol)(H_2O)_4^+$. Several structures have been calculated at the UHF level, but only a selected number of cluster geometries are calculated at the MP2 and DFT levels. In the case of $(phenol)(H_2O)_4^+$, no MP2 calculations were performed, and no BSSE corrections were taken into account for all $(phenol)(H_2O)_{n>1}^+$ clusters. In this paper, ROHF calculations (6-31G(d,p) basis) are presented for several structures of $(phenol)(H_2O)_{1-4}^+$ applying the Gaussian program.[18] By using the ROHF method, spin contaminations are avoided. Additionally, a unique scaling factor for all OH vibrations of all cluster sizes can be chosen. All calculated stabilization energies are BSSE corrected using the counterpoise method of Boys and Bernardi.[19] Zero point energy (ZPE) corrections are performed by using the unscaled harmonic frequencies. For each cluster size, the results of our calculations will be compared with the results obtained by Re and Osamura[17] (see below).

In case of the $(phenol)(H_2O)_1^+$ and $(phenol)(H_2O)_2^+$ clusters, only one minimum energy structure has been found. The structure of $(phenol)(H_2O)_1^+$ contains a trans-linear arrangement of phenol and water.[20] In the case of $(phenol)(H_2O)_2^+$, phenol is hydrogen bonded to a water dimer. All intermolecular hydrogen bonds (phenol−water, water−water) are trans-linear. The UHF, UMP2, and DFT calculations presented in ref 17 lead to the same result. In contrast to the S_0 state,[21] no cyclic structure of $(phenol)(H_2O)_2^+$ turns out to be stable. Furthermore, no stable van der Waals complex could be obtained. Especially structures with one or two water molecules located above the aromatic ring turn out to be not stable.

Several minimum energy structures are obtained for $(phenol)(H_2O)_3^+$ and $(phenol)(H_2O)_4^+$ clusters. Similar to $(phenol)(H_2O)_1^+$ and $(phenol)(H_2O)_2^+$, one local minimum energy structure is a linear arrangement ("type III") forming a chain of phenol and water moieties (cf. Figure 1). Another structural arrangement is a "solvated cluster". Concerning this structure, each hydrogen atom of the first water molecule (hydrogen-bonded to phenol) undergoes a hydrogen bond to another water molecule. These additional water molecules form the first solvation shell in $(phenol)(H_2O)_3^+$. In the case of $(phenol)(H_2O)_4^+$, the fourth water molecule starts to build up the second solvation shell (cf. Figure 1). In the solvated structures of the $(phenol)(H_2O)_{3,4}^+$ clusters, proton transfer between the OH group of phenol and the first water molecule can occur; i.e., both a proton-transfer structure (type II) and a nonproton-transfer structure (type I) turn out to be local minima on the PES. In case of $(phenol)(H_2O)_4^+$, a cyclic arrangement with PT (see Figure 1f, type IV) represents another local minimum energy structure. The relative stabilities of all structures (types I−IV) are given in Table 1. It has to be mentioned that all calculations are performed by using a double-ζ basis set and no correlation energies are taken into account. Thus, the stabilization energies calculated at the ROHF/6-31G(d,p) level can only be taken as an indication of the most stable arrangement. From the values given in Table 1, it can be concluded that in the case of $(phenol)(H_2O)_3^+$ the type I structure is the most stable arrangement, whereas the proton-transfer structure (type II) is less stable. Additionally, the linear configuration (type III) has to be taken

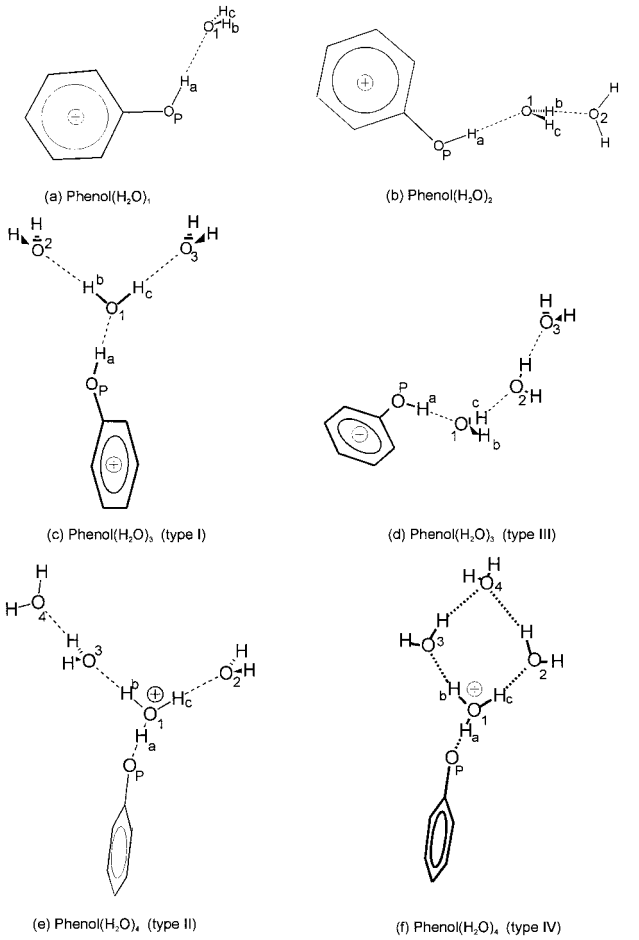

Figure 1. Most stable structures of the $Ph(H_2O)_{1-4}$ cations. Three minimum energy structures are found for the $Ph(H_2O)_3^+$ cluster, and four minimum energy structures are discussed for the $Ph(H_2O)_4^+$ cluster (see Table 1). The most stable structures of $Ph(H_2O)_3^+$ are the solvated structure without proton transfer (type I, see c) and the linear configuration (type III, see d). In the case of $Ph(H_2O)_4^+$, the solvated structure with proton transfer (type II, see e) and the cyclic structure (type IV, see f) are shown.

TABLE 1: Relative Stabilities of Minimum Energy Structures of (Phenol)$(H_2O)_3^+$ and (Phenol)$(H_2O)_4^+$ [a]

structure	(phenol)$(H_2O)_3^+$	(phenol)$(H_2O)_4^+$
I	0	143
II	513	0
III	528	1033
IV		404

[a] All values (in cm^{-1}) are corrected by the BSSE[19] and the zero-point energy. I and II refer to the solvated structures without and with proton transfer, respectively (see Figure 1c and e). III represents a linear structure (see Figure 1d). IV represents a cyclic structure with proton transfer (see Figure 1f).

into account. In the case of (phenol)$(H_2O)_4^+$, the linear structure becomes less stable compared to the corresponding structure of (phenol)$(H_2O)_3^+$. The noncyclic proton-transfer structure (type II) is the most stable arrangement for (phenol)$(H_2O)_4^+$.

In contrast to our calculations, the UHF calculations given in ref 17 predict that the type II structure of (phenol)$(H_2O)_3^+$ is more stable than the type I structure. UMP2 and DFT calculations are not given for both structures. A comparison with the experimental results is given in section IV. In the case of (phenol)$(H_2O)_4^+$, the type II structure has not been discussed by Re and Osammura.[17] They presented the cyclic proton-transfer structure (type IV) as the most stable arrangement. From

TABLE 2: Geometrical Parameter of Calculated Minimum Energy Structures of (Phenol)$(H_2O)_{1-4}$ Cations[a]

			$Ph(H_2O)_3^+$		
	$Ph(H_2O)_1^+$	$Ph(H_2O)_2^+$	I	III	$Ph(H_2O)_4^+$ (II)
R(P,1)	2.667	2.585	2.522	2.558	2.487
R(1,2)		2.781	2.817	2.709	2.550
R(1,3)			2.817	5.011	2.653
R(2,3)			4.626	2.845	4.334
R(3,4)					2.793
r(P,a)	0.972	0.985	1.003	0.991	1.478
r(1,a)	1.695	1.602	1.511	1.569	1.010
r(1,b)	0.946	0.959	0.956	0.964	0.990
r(1,c)	0.946	0.945	0.956	0.945	0.972

[a] Concerning the labels 1−4 and a, b, c, P, see Figure 1. All values in Ångstroms.

the calculated stabilization energies at the ROHF level and from the comparison between the calculated and experimentally observed vibrational frequencies and intensities, it can be concluded that a noncyclic structure (type II or type I) is the most stable arrangement (see section IV).

For the most stable structures of the (phenol)$(H_2O)_{1-4}^+$ clusters, both the intermolecular distances (distances between the O atoms) and the OH bond lengths of phenol and the first water molecule are listed in Table 2. As expected, the OO bond lengths are shorter in a region where proton transfer can take place (cf. geometrical parameters of phenol and the first water molecule). Additionally, the OH bond length (*r(P,a)*) increases if an OH group is involved in a PT coordinate.

The calculated OH frequencies and experimental values are listed in Table 3 (see discussion in section IV).

(IV) Experimental Results and Discussion

Figure 2 displays the resonant two-color, two-photon ionization spectra of (phenol)$(H_2O)_{1-4,7,8}$. The bands used for analysis of infrared photodissociation are marked with an asterisk. The assignment of the spectral features to cluster structures and vibrations in the electronic ground state is presented elsewhere.[22,23] In short, the $n = 1$ cluster has nearly a linear H bond with trans positions of the H atoms of H_2O relative to the aromatic ring.[23] The $n = 2-4$ clusters form cyclic structures.[23] The $n = 7$ and $n = 8$ isomers marked in Figure 2 have structures based on the cubic $(H_2O)_8$ arrangement.[22] In the (phenol)$(H_2O)_7$ cluster, one H_2O in the cube of $(H_2O)_8$ is replaced by phenol (isomers B and C). In the (phenol)$(H_2O)_8$ cluster, phenol is inserted into an edge of the cube (isomer B) or phenol is hydrogen-bonded to the $(H_2O)_8$ cube (isomer A).[22]

The ionization potentials of the clusters up to $n = 12$ are presented in Figure 3 together with the experimental uncertainties that result mainly from the slow rise of the ionization threshold of the larger clusters (cf. section II). UV hole-burning experiments prove that different isomers of the $n = 7$ and $n = 8$ clusters are formed in the jet.[22] These isomers have different ionization thresholds; see Figure 3 and Table 4. The experimentally observed ionization thresholds decrease with increasing cluster size at least up to $n = 7$ or 8.

In Figure 4, the fragmentation threshold of the process (phenol)$(H_2O)_n \rightarrow$ (phenol)$(H_2O)_{n-1} + H_2O$ is given as a function of the cluster size n. The stability of the clusters decreases with increasing n. Since the proton affinity of water increases with the cluster size, a proton-transfer structure becomes the most stable arrangement for larger (phenol)$(H_2O)_n^+$ clusters. Starting from a nonproton transfer form in the S_1 state (after excitation from the S_0 to the S_1 state), the cluster species

TABLE 3: Experimentally Observed Frequencies of the OH Stretching Vibrations of (a) $Ph(H_2O)_{1-4}^+$ and (b) $Ph(H_2O)_{3,4}^+$ Compared to the Calculated OH Stretching Frequencies of the (a) Linear and (b) Solvated Structures[a]

Section a

	$Ph(H_2O)_1^+$		$Ph(H_2O)_2^+$		$Ph(H_2O)_3^+$		$Ph(H_2O)_4^+$
	calcd	exptl	calcd	exptl	calcd	exptl	calcd
ν(POH)	3158	n.o.	2903	n.o.	2787	n.o.	2733
$\nu(H_2O$, sym, t)	3608	3626	3628	3634	3632	3642	3634
$\nu(H_2O$, asym, t)	3699	3709	3722	3704	3729	3729	3733
ν(OH, free, $t-1$)			3673	3680	3699	3681?	3704
ν(OH, bound, $t-1$)			3431	n.o.	3521	n.o.	3549
ν(OH, free, $t-2$)					3674	3681?	3698
ν(OH, bound, $t-2$)					3317	n.o.	3454
ν(OH, free, $t-3$)							3675
ν(OH, bound, $t-3$)							3267

Section b

	$Ph(H_2O)_3^+$			$Ph(H_2O)_4^+$			
	calcd			calcd			
assignment	I	II	exptl	I	II	exptl	assignment
ν(OH, a)	2552	2079	n.o.	2387	2442	n.o.	ν(OH, a)
ν(OH, b−c, sym)	3458	3147	n.o.	3384	3182	n.o.	ν(OH, b)
ν(OH, b−c, asym)	3516	3152	n.o.	3503	2898	n.o.	ν(OH, c)
$\nu(H_2O$, 2−3, sym)(1)	3630	3623	3642	3631	3625	3643	$\nu(H_2O$, 2, sym)
$\nu(H_2O$, 2−3, asym)(1)	3727	3719	3729	3728	3721	3725	$\nu(H_2O$, 2, asym)
$\nu(H_2O$, 2−3, sym)(2)	3630	3624	3642	3633	3630	3643	$\nu(H_2O$, 4, sym)
$\nu(H_2O$, 2−3, asym)(2)	3727	3719	*b*	3731	3727	3725	$\nu(H_2O$, 4, asym)
$\nu(H_2O$, 3, bound)				3538	3466	≈3400	$\nu(H_2O$, 3, bound)
$\nu(H_2O$, 3, free)				3701	3694	3698	$\nu(H_2O$, 3, free)

[a] All values are given in cm^{-1}. *t* represents the terminal water molecule with two free OH groups. Water molecule $t-1$ is hydrogen-bonded to the terminal water molecule; water molecules $t-2$ and $t-3$ are hydrogen-bonded to $t-1$ and $t-2$, respectively. n.o. = not observed. I: nonproton-transfer solvated structure; see Figure 1c. II: proton-transfer solvated structure; see Figure 1e. All calculated frequencies are scaled by a factor of 0.876. [b] This vibration cannot be observed due to negligible IR intensity.

are ionized by an UV photon. After relaxation to the proton-transfer form in the D_0 state, the resulting excess energy diminishes the apparent dissociation energy. This leads to a decrease of the fragmentation thresholds with increasing *n* (see Figure 4 and Table 4).

All experimentally observed OH stretching vibrations in the IR spectra of $(phenol)(H_2O)_n^+$ are listed in Table 5. The bandwidths are given, too.

Figure 5 presents the IR spectra of $(phenol)(H_2O)_{1-3}^+$ in the spectral range from 2850 to 3800 cm^{-1}. In case of the $n = 1$ cluster ion, IR photodissociation can be observed if the cluster is ionized by a one-color R2PI process via the electronic origin of the $S_1 \leftarrow S_0$ transition (total energy: 71 998 cm^{-1}). By using the third harmonic of a Nd:YAG laser (355 nm) as the second color in a $(1 + 1')$ R2PI process (total energy: 64 168 cm^{-1}), no fragmentation of $(phenol)(H_2O)_1^+$ is observed due to the small ion excess energy of 144 cm^{-1}. In the case of $(phenol)(H_2O)_{1-3}^+$, we observe similar spectra as those presented in ref 12 with respect to vibrational frequencies and bandwidth. The signal-to-noise ratio of our spectra is better, which allows the detection of weak transitions and the deconvolution of overlapping bands. The similar bandwidths in the jet-cooled spectra of ref 12 and in our spectra indicate that our spectra are not internally hot with respect to the water moiety of the cluster.

In Figure 5a, the IR photodissociation spectrum of $(phenol)(H_2O)_1^+$ is shown. Two vibrations at 3626 and 3709 cm^{-1} are observed. These frequencies fit very well the calculated values of the symmetric and antisymmetric OH stretching frequencies at 3608 and 3699 cm^{-1} (cf. Table 3a). In the IR/R2PI spectrum of neutral $(phenol)(H_2O)_1$ (S_0 state),[23] the ν_1 transition is too weak to be observed. Compared to this spectrum, the ν_1 band in the IR photodissociation spectrum performed for the D_0 state is very intense and even more intense than the ν_3 transition. The calculated intensity ratio for the ν_1 and ν_3 vibrations in the D_0 state is 1:2. The intensity ratio for the S_0 state is 1:5; i.e., the gain in intensity observed for the ν_1 vibration in the D_0 state is qualitatively predicted by the ab initio calculations. The very large experimental intensity of the ν_1 vibration may be attributed to a perturbing effect of the nearby positive charge on the aromatic ring.

The phenolic OH stretching vibration of $(phenol)(H_2O)_1^+$ can be expected in a range roughly around 3150 cm^{-1}, cf. section III, but it is not observed in our IR photodissociation spectra, although the IR intensity should be larger than those of the ν_1 and ν_3 vibrations. The phenolic OH stretching vibration may be extremely broad due to the flat potential of the proton-transfer coordinate or the excitation of this transition does not lead to an efficient H_2O fragmentation.

The IR photodisscociation spectrum of $(phenol)(H_2O)_2^+$ is given in Figure 5b. The electronic origin of the $S_1 \leftarrow S_0$ transition at 36 228 cm^{-1} of the $(phenol)(H_2O)_2$ cluster is broad, and the R2PI signal is relatively small. Thus, the intensity of signals in the IR photodissociation spectra of $(phenol)(H_2O)_2^+$ is lower compared to the signals of the spectra of $(phenol)(H_2O)_{1,3,4,7,8}^+$. The IR photodissociation spectrum of $(phenol)(H_2O)_2^+$ shows an antisymmetric broad band with a peak at 3681 cm^{-1} (see Figure 5b). This band can be deconvoluted into two transitions at 3680 and 3704 cm^{-1}. Furthermore, a weak transition at 3634 cm^{-1} is observed. If we assume a linear structure of $(phenol)(H_2O)_2^+$ (see section III), a good correlation between the calculated and experimentally observed frequencies can be achieved (see Table 3a). The vibrational transitions at 3634 and 3704 cm^{-1} represent the symmetric and antisymmetric OH stretching vibrations of the free water molecule of $(phenol)(H_2O)_2^+$. The transition at 3680 cm^{-1} can be assigned to the

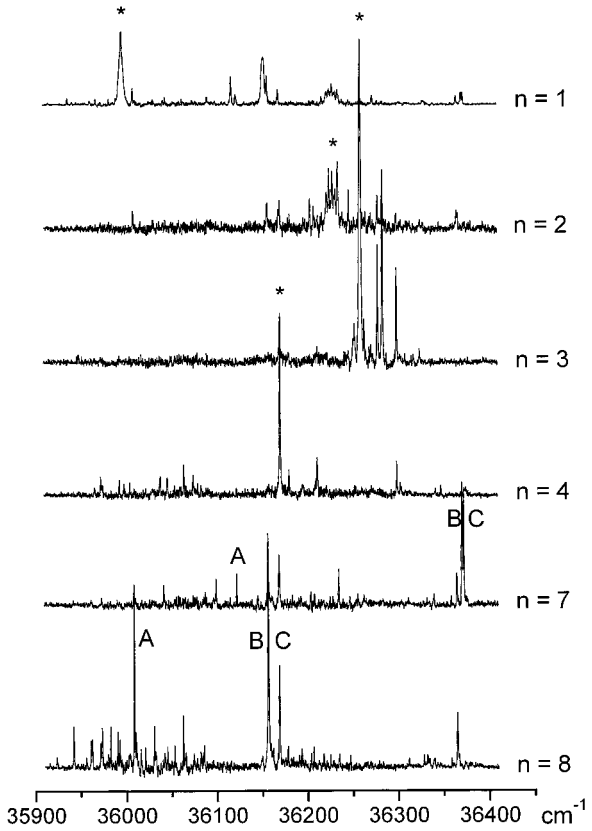

Figure 2. Resonant two-photon ionization spectra of $Ph(H_2O)_n^+$ ($n = 1-4$, 7, 8) obtained via two-color excitation ($\lambda_1 + 355$ nm). The bands marked with an asterisk are used for IR-PARI. The intensities in the R2PI spectra are falsified due to laser saturation effects. The bands marked with letters stem from different isomers of the $n = 7$ and $n = 8$ clusters as revealed by UV spectral hole burning.[22] The bands B and C of the $n = 7$ cluster and band B of the $n = 8$ cluster are used for IR-PARI.

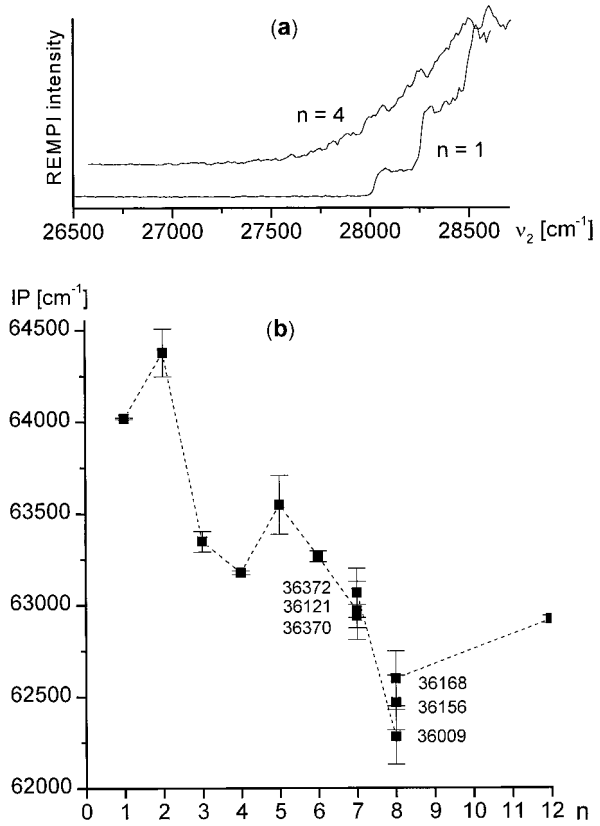

Figure 3. Ionization thresholds of phenol/water clusters. (a) Example of a steep rise of the ionization threshold for $n = 1$ with steps from vibrational excitation of the ion. In the case of $n = 4$, a slow rise of the ionization threshold is obtained. (b) The ionization thresholds of $(phenol)(H_2O)_n^+$ clusters up to $n = 12$ together with their error bars. The displayed numbers indicate the $S_1 \leftarrow S_0$ transitions of different isomers of the $n = 7$ and $n = 8$ clusters (in cm^{-1}). The phenol monomer has an ionization potential of 68 623 cm^{-1}.[16] ZEKE experiments lead to an adiabatic ionization potential of 64 024 ± 5 cm^{-1} for the $n = 1$ cluster.[16]

OH stretching vibration of the free OH group of the first water molecule, which is hydrogen-bonded to the phenol moiety.

In the case of the $(phenol)(H_2O)_3^+$ cluster, three peaks at 3642, 3681, and 3729 cm^{-1} can be observed in the IR photodissociation spectrum (see Figure 5c). According to the ab initio calculations (see section III), the most stable structure of $(phenol)(H_2O)_3^+$ turns out to be a solvated arrangement without PT (type I). The frequencies calculated for the symmetric (3630 cm^{-1}) and antisymmetric OH stretching vibrations (3727 cm^{-1}) of the free water molecules fit the experimental frequencies at 3642 and 3729 cm^{-1}.

The weak transition at 3681 cm^{-1} can only be explained if the linear structure of $(phenol)(H_2O)_3^+$ is also taken into account (see Figure 1d). Assuming this structure, the transition at 3681 cm^{-1} can be interpreted as the OH stretching frequency of the free OH group of one of the hydrogen-bonded water molecules. The transitions at 3642 and 3729 cm^{-1} can be correlated with the symmetric and antisymmetric OH stretching vibrations of the free water molecule of the linear structure.

The transitions at 3642 and 3729 cm^{-1} are much more intense than the transition at 3681 cm^{-1}, whereas the transition at 3681 cm^{-1} is very intense in the spectrum of $(phenol)(H_2O)_2^+$. With respect to these experimental results, it can be concluded that both the solvated structure and a linear arrangement of $(phenol)(H_2O)_3^+$ are formed in our molecular beam. The solvated structure (type I or type II) is supposed to be the most stable arrangement.

With respect to the calculated OH stretching frequencies of the free water molecules, it is not possible to distinguish between a type I and a type II structure (see Table 3b). Unfortunately, no OH stretching vibrations from the first water molecule (type I structure) or from the hydronium ion (type II structure) are observed. This may result from a very flat potential along the proton-transfer coordinate, leading to broad transitions for all OH stretching vibrations of the a, b, and c OH groups (see Figure 1). A very efficient IVR after excitation of the OH stretching vibrations of the a, b, and c OH groups may also be a reason why these vibrations cannot be observed in the IR photodissociation spectrum. The experimentally measured ex-

TABLE 4: Experimentally Observed Ionization Potentials and Fragmentation Potentials; Standard Deviations of Repeated Measurements Are Given

n	$S_1 \leftarrow S_0$, cm^{-1}	IP, cm^{-1}	FP, cm^{-1}
1	35 997	64 019 ± 5	*a*
2	36 228	64 380 ± 130	66 750 ± 15
3	36 259	63 350 ± 60	65 740 ± 130
4	36 169	63 180 ± 10	64 160 ± 40
5	36 299	63 550 ± 160	64 390 ± 25
6	36 348	63 270 ± 30	63 710 ± 55
7	36 121	62 970 ± 160	63 840 ± 35
7	36 370	62 940 ± 65	64 290 ± 80
7	36 372	63 070 ± 135	64 390 ± 95
8	36 009	62 280 ± 150	63 990 ± 80
8	36 156	62 470 ± 150	63 750 ± 80
8	36 168	62 600 ± 150	63 540 ± 140
12	35 972	62 920 ± 20	63 840 ± 10

[a] See Figure 4b.

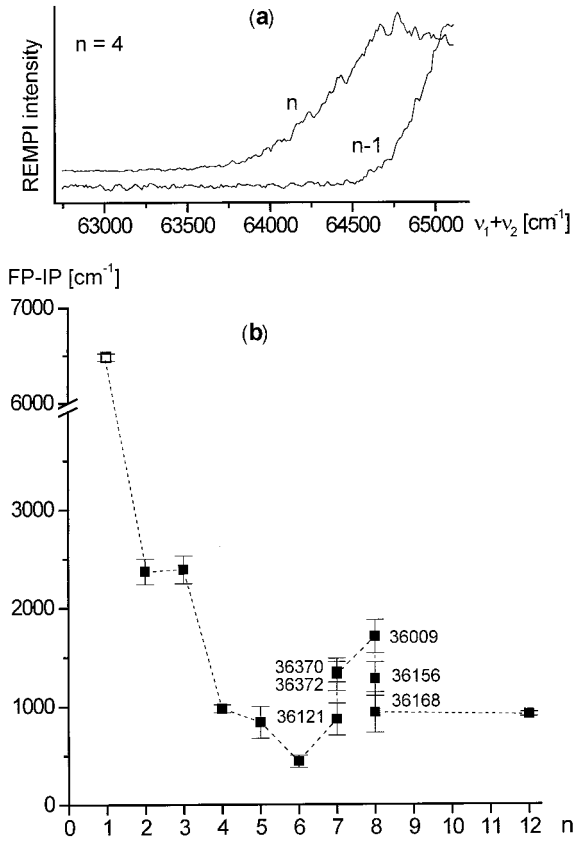

Figure 4. (a) Threshold rise of the parent ion signal $(phenol)(H_2O)_4^+$ and its fragment $(phenol)(H_2O)_3^+$. (b) Excess energy necessary for fragment appearance in $(phenol)(H_2O)_{1-12}^+$. The displayed numbers indicate the band positions of different isomers (in cm^{-1}). The $n = 7$ cluster ions with a filled second solvation shell and the $n = 8$ isomers obtained via $S_1 \leftarrow S_0$ excitation at 36 009 and 36 156 cm^{-1} are remarkably stable compared to the other clusters with $n \geq 4$. The value for $(phenol)(H_2O)_1^+$ is taken from ref 25.

cess energies that lead to a fragmentation of the cluster ions (see below and Figure 4b) are still quite large for $n = 3$ and support the assumption that the nonproton-transfer structure (type I) is the most stable arrangement of the $(phenol)(H_2O)_3^+$ cluster at least on the time scale of our experiment (40 ns). The electronic spectra of $(phenol)(H_2O)_{n=1-4}^+$ obtained in ref 11 are broad and essentially unstructured for $n = 1-3$. This is typical for an electronic spectrum of $(phenol)^+$, indicating that no proton transfer occurs in $(phenol)(H_2O)_{n=1-3}^+$. The spectrum of $(phenol)(H_2O)_4^+$ is similar to the spectrum of the phenoxy radical, which has a rich vibronic structure; i.e., proton transfer occurs in the $n = 4$ cluster. In the spectrum of $(phenol)(H_2O)_3^+$, the broad band is superimposed by some sharp transitions belonging to the absorption of the phenoxy radical. Thus, the authors conclude that proton transfer already takes place for $(phenol)(H_2O)_3^+$.[11] Our measurements of the fragmentation energies do not indicate a significant proton transfer for the $n = 3$ cluster. In contrast to our measurements, the ion-trap experiment of ref 11 is in the millisecond regime and significant proton transfer may occur on that time scale for $(phenol)(H_2O)_3^+$.

In contrast to ref 12, we are able to obtain mass-selected IR spectra of $(phenol)(H_2O)_{4,7,8}^+$. In Figure 6a, the IR photodissociation spectrum of $(phenol)(H_2O)_4^+$ obtained via UV excitation of the electronic origin at 36 170 cm^{-1} is given. The vibrations at 3643 and 3725 cm^{-1} can be interpreted as symmetric and antisymmetric OH stretching vibrations of the free water molecules (cf. Table 3 and Table 5). The very broad band at about 3390 cm^{-1} indicates that the second solvation shell is formed. From the ROHF calculations it can be expected that the OH stretching frequency of the hydrogen-bonded OH group (between the first and second solvation shells) is about 3400 cm^{-1}. This is in agreement with the experimental results.

TABLE 5: Experimental Frequencies and Bandwidths

n	IR freq, cm^{-1}	Lorentzian FWHM, cm^{-1}
1	3626	9.2 (*n*) 9.0−9.2 (*n* − 1)
	3709	26 (*n*) 18−21 (*n* − 1)
2	3634 ± 0.6[b]	38 ± 2[b]
	3680 ± 0.3[b]	26 ± 1[b]
	3704 ± 1[b]	42 ± 3[b]
3[a]	3642	11.5−11.8 (*n*) 10.8−11.3 (*n* − 1)
	3681	9−11 (*n*)
	3728−3731	22−28 (*n*) 25−28 (*n* − 1)
4	3380−3400	140−150
	3643 ± 0.1[c]	16 ± 1[c]
	3698 ± 1[c]	22 ± 2[c]
	3725 ± 1[c]	36 ± 3[c]
7 (36 170)	3450−3460	140−150
	3647	11
	3710−3714	21−33
8 (36 156)	ca. 3430	≈210
	3711−3713	28

[a] One- and two-color experiments. [b] Fitted as three Lorentzians with fully relaxed parameters. [c] Fitted as two Lorentzians with fully relaxed parameters; fit has been performed for trace *n*.

By comparing the experimentally observed frequencies of the OH vibrations with the calculated values for the cyclic $(phenol)(H_2O)_4^+$ cluster (type IV), the agreement between experimental and theoretical results is much less satisfactory than for the type I and type II structures. The calculated frequencies (scaled by a factor of 0.876) of the antisymmetric stretching vibration of $H_2O(4)$ and the free OH groups of $H_2O(2)$ and $H_2O(3)$ (see Figure 1f) are very close together (3696, 3700, and 3704 cm^{-1}). In contrast to this result, the corresponding calculated frequencies of the type II/type I structures (3694/3701, 3721/3728, and 3727/3731 cm^{-1}; see Table 3) are separated by about 30 cm^{-1}, which fits very well with the experimental results (experimental frequencies at 3698 and 3725 cm^{-1}; see Table 3). The frequencies of the symmetric stretching vibrations of $H_2O(2)$ and $H_2O(4)$ in the type I and type II structures are nearly identical. The sum of the calculated intensities of these vibrations is similar to the intensity of an antisymmetric stretching vibration. This agrees with the experimental result (see Figure 6a). The calculated intensity of the symmetric stretching vibration (3606 cm^{-1}) of $H_2O(4)$ in the type IV structure is by a factor of 10 smaller than the calculated intensity of an antisymmetric stretching vibration. Furthermore, the calculated frequencies of the bound OH groups of $H_2O(2)$ and $H_2O(3)$ (3556 and 3565 cm^{-1}) are about 100 cm^{-1} higher than the corresponding value of the type II structure (3466 cm^{-1}; see Table 3). The value obtained for the type II structure fits the experimental value of about 3400 cm^{-1} much better. From all comparisons between the calculated and experimental frequencies, it can be concluded that the type IV structure cannot be observed under our experimental conditions.

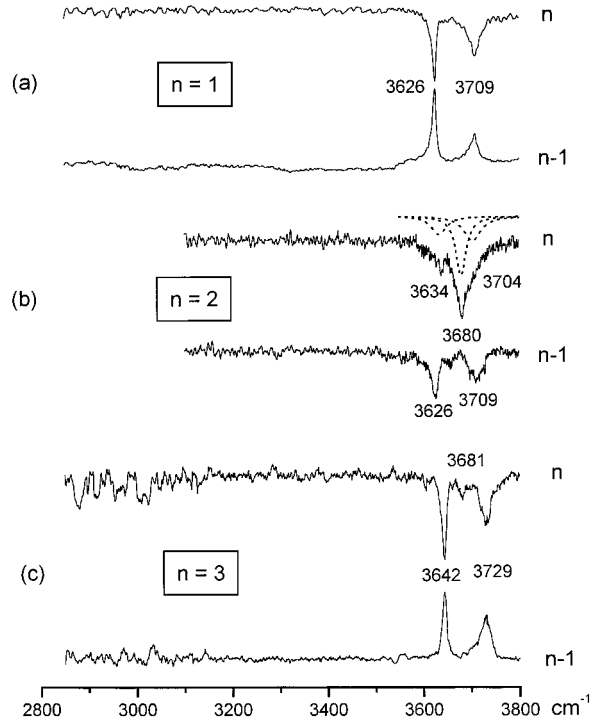

Figure 5. Infrared photodissociation spectra of (phenol)$(H_2O)_{1-3}^+$ produced via resonant one-color excitation for $n = 1$ and 2 and two-color excitation ($\lambda_1 + 355$ nm) for $n = 3$. Both the IR ion photodissociation spectrum at the mass of the cluster parent and the corresponding rise of the $-H_2O$ fragment signal are given. If ionizing with one-color excitation, considerable $-H_2O$ fragmentation occurs. According to this fragmentation, $n - 1$ fragment ions are formed and the $n - 1$ IR frequencies can be seen as dips in the $n - 1$ fragment spectrum of the cluster of size n, cf. the $n = 2$ spectra.

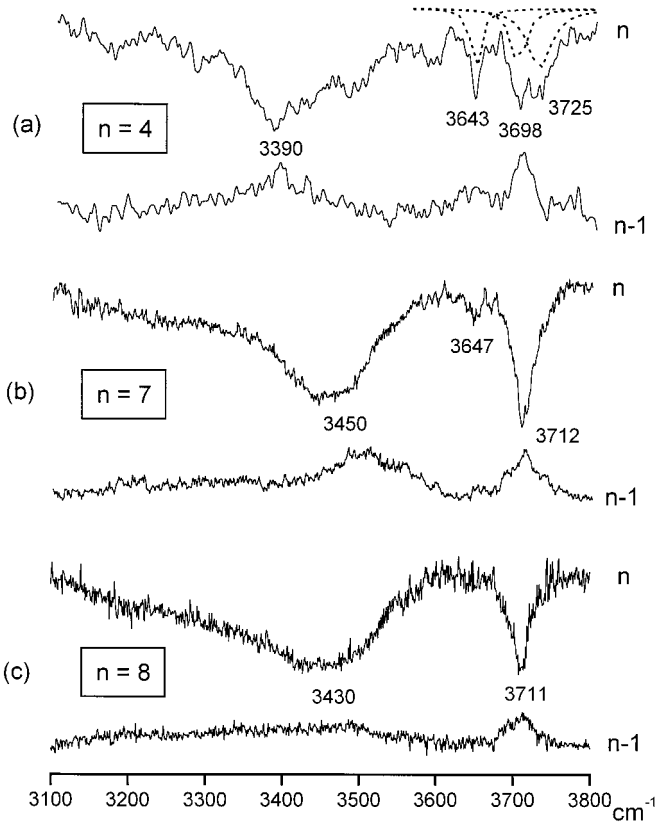

Figure 6. Infrared photodissociation spectra of (phenol)$(H_2O)_{4,7,8}^+$ produced via resonant two-color excitation ($\lambda_1 + 355$ nm). The dips in parent ion intensity from IR photodissociation and the corresponding rise of the $-H_2O$ fragment signals are shown.

Similar to the (phenol)$(H_2O)_3^+$ cluster, it is not possible to decide whether the type I or type II structure of (phenol)$(H_2O)_4^+$ is more stable if only the frequencies of the OH stretching vibrations are taken into account (cf. Table 3). To get more information on the stability of the different structures, the results of the fragmentation potential measurements should be taken into account. The excess energies (FP − IP) of (phenol)$(H_2O)_2^+$ and (phenol)$(H_2O)_3^+$ are about 2400 cm^{-1} (see Table 4 and Figure 3). In the case of (phenol)$(H_2O)_4^+$, the excess energy is about 1000 cm^{-1}; i.e., there is a substantial change in the structure by going from (phenol)$(H_2O)_3^+$ to (phenol)$(H_2O)_4^+$. Thus, it can be concluded that the nonproton-transfer structure (type I) is the most stable arrangement for (phenol)$(H_2O)_3^+$ under our experimental conditions, whereas the proton-transfer structure (type II) is the most stable arrangement for (phenol)-$(H_2O)_4^+$. This conclusion is in good agreement with the results of the ab initio calculations (see section III). The ROHF calculations show that the proton-transfer structure becomes the most stable structure by going from (phenol)$(H_2O)_3^+$ to (phenol)$(H_2O)_4^+$.

In parts b and c of Figure 6, the IR photodissociation spectra of (phenol)$(H_2O)_7^+$ and (phenol)$(H_2O)_8^+$ are shown. The spectra are obtained via the S_1 transitions at 36 370 ((phenol)$(H_2O)_7^+$) and 36 156 cm^{-1} ((phenol)$(H_2O)_8^+$). The IR spectrum observed via the electronic origin (36 372 cm^{-1}) of a second isomer of the (phenol)$(H_2O)_7^+$ cluster is identical to the spectrum shown in Figure 6b. The peak positions differ only by 2 cm^{-1}. The IR spectra given in parts b and c of Figure 6 show transitions at 3647 and 3712 cm^{-1} and a broad transition at about 3450 cm^{-1}. With respect to the calculations performed for the (phenol)-$(H_2O)_4^+$ cluster and by comparing these results with the one obtained for the pure water clusters,[9,10] it can be concluded that the fifth, sixth, and seventh water molecules fill up the second solvation shell. It is also possible that the third solvation shell is formed before the second solvation shell is full. This may lead to different isomers of the (phenol)$(H_2O)_7^+$ cation. However, in the case of (phenol)$(H_2O)_8^+$, the third solvation shell will be formed by at least one water molecule. The transitions at 3712 cm^{-1} in the (phenol)$(H_2O)_{7,8}^+$ clusters can be interpreted as the antisymmetric OH stretching vibration of the free water molecules. The transition at 3647 cm^{-1} of the (phenol)$(H_2O)_7^+$ cluster can be assigned to the corresponding ν_1 vibration. The intensity of the ν_1 vibrations decreases considerably with increasing cluster size. This may result from the larger distance of the outer water molecules from the perturbing positive charge.

The broad transition at 3450 cm^{-1} results from the OH stretching vibrations of the free OH groups of the water molecules, which undergo hydrogen bonds between the first and second or the second and third solvation shells.

(V) Conclusions

The infrared spectra of the (phenol)$(H_2O)_n^+$ cluster ($n = 1-4$, 7, 8) have been obtained for the OH stretching vibrations by applying the IR-PARI technique. Using this method, the different cluster species are formed via resonant two-photon ionization. The OH stretching vibrations of the ions are resonantly excited, and the cluster photodissociates by loss of one water molecule. The experimentally observed frequencies are compared with the results of the ROHF calculations. From

the IR spectra, the ab initio calculations, and the measurements of the fragmentation potentials, the most stable structures of the cluster ions have been derived. The structure of (phenol)$(H_2O)_1^+$ is trans-linear. (Phenol)$(H_2O)_2^+$ is not cyclic but linear. (Phenol)$(H_2O)_3^+$ probably forms both a linear and a solvated structure. The most stable arrangement is supposed to be a solvated structure without proton transfer. For (phenol)$(H_2O)_4^+$, the most stable structure is a solvated arrangement with proton transfer between phenol and the first hydrogen-bonded molecule. In the case of (phenol)$(H_2O)_{4,7,8}^+$, the second and third solvation shells are at least partially filled, indicated by a broad transition in the IR spectra at about 3400 cm^{-1}.

IR-PARI is especially suited to study ions that undergo large structural changes (e.g., proton-transfer reactions) after resonant ionization. Furthermore, time-resolved measurements of chemical reactions in ions can be performed. IR-PARI is energy and product state selective. The method is not state selective with respect to the educt like the IR−PIRI method,[24] which in turn requires the existence of long-lived Rydberg states.

Acknowledgment. We thank the Deutsche Forschungsgemeinschaft for financial support. Ch. J. thanks the Fond der Chemischen Industrie for financial support.

Addendum

After submission of this paper, Piest et al. published IR photodissociation spectra of resonantly ionized anilin−Ar^+ using a free electron laser.[26]

References and Notes

(1) (a) Eigen, M. *Angew. Chem., Int. Ed. Engl.* **1964**, *3*, 1. (b) Ratcliffe, C.; Irish, D. E. In *Water Science Reviews*; Franks, F., Ed.; Cambridge University Press: Cambridge, 1986; p 149.

(2) (a) Okumura, M.; Yeh, L. I.; Lee, Y. T. *J. Chem. Phys.* **1985**, *83*, 3705; **1988**, *88*, 79. (b) Okumura, M.; Yeh, L. I.; Myers, J. D.; Lee, Y. T. *J. Chem. Phys.* **1986**, *85*, 2328. (c) Liu, W. L.; Lisy, J. M. *J. Chem. Phys.* **1988**, *89*, 605.

(3) Yeh, L. I.; Okumura, M.; Myers, J. D.; Price, J. M.; Lee, Y. T. *J. Chem. Phys.* **1989**, *91*, 7319.

(4) Okumura, M.; Yeh, L. I.; Myers, J. D.; Lee, Y. T. *J. Phys. Chem.* **1990**, *94*, 3416.

(5) Crofton, M. W.; Price, J. M.; Lee, Y. T. IR Spectroscopy of Hyrogen Bonded Charged Clusters. In *Clusters of Atoms and Molecules II*; Haberland, H., Ed.; Springer: Berlin, 1994; p 44.

(6) (a) Robinson, G. W.; Thistlethwaite, P. J.; Lee, J. *J. Phys. Chem.* **1986**, *90*, 4224. (b) Lee, J.; Robinson, G. W.; Webb, S. P.; Phillips, L. A.; Clark, J. H. *J. Am. Chem. Soc.* **1986**, *108*, 6538.

(7) Narcisi, R. S.; Bailey, A. D. *J. Geophys. Res.* **1965**, *70*, 3687.

(8) Ferguson, E. E.; Fehsenfeld, F. C.; Albritton, D. L. In *Gas Phase Ion Chemistry*; Bowers, M. T., Ed.; Academic: New York, 1979; Vol. 1, p 45.

(9) (a) Newton, M. D. *J. Chem. Phys.* **1977**, *67*, 5535. (b) Remington, R.; Schaefer, H. F. Unpublished results, quoted in ref 3.

(10) Wei, D.; Salahub, D. R. *J. Chem. Phys.* **1994**, *101*, 7633.

(11) Sato, S.; Mikami, N. *J. Phys. Chem.* **1996**, *100*, 4765.

(12) Sawamura, T.; Fujii, A.; Sato, S.; Ebata, T.; Mikami, N. *J. Phys. Chem.* **1996**, *100*, 8131.

(13) (a) Jacoby, C.; Roth, W.; Schmitt, M.; Janzen, C.; Spangenberg, D.; Kleinermanns, K. *J. Phys. Chem. A* **1998**, *102*, 4471. (b) Schmitt, M.; Jacoby, C.; Kleinermanns, K. *J. Chem. Phys.* **1998**, *108*, 4486.

(14) Marchand, P.; Marmet, L. *Rev. Sci. Instrum.* **1983**, *54*, 1034.

(15) (a) Chupka, W. A. *J. Chem. Phys.* **1993**, *98*, 4520. (b) Chupka, W. A. *J. Chem. Phys.* **1993**, *99*, 5800.

(16) Dopfer, O.; Reiser, G.; Müller-Dethlefs, K.; Schlag, E. W.; Colson, S. D. *J. Chem. Phys.* **1994**, *104*, 974.

(17) Re, S.; Osamura, Y. *J. Phys. Chem. A* **1998**, *102*, 3798.

(18) Frisch, M. J.; Trucks, G. W.; Schlegel, H. B.; Gill, P. M. W.; Johnson; B. G.; Robb, M. A.; Cheeseman, J. R.; Keith, T.; Petersson, G. A.; Montgomery, J. A.; Raghavachari, K.; Al-Laham, M. A.; Zakrzewski, V. G.; Ortiz, J. V.; Foresman, J. B.; Cioslowski, J.; Stefanov, B. B.; Nanayakkara, A.; Challacombe, M.; Peng, C. Y.; Ayala, P. Y.; Chen, W.; Wong, M. W.; Andres, J. L.; Replogle, E. S.; Gomperts, R.; Martin, R. L.; Fox, D. J.; Binkley, J. S.; Defrees, D. J.; Baker, J.; Stewart, J. P.; Head-Gordon, M.; Gonzalez, C.; Pople, J. A. Gaussian, Inc., Pittsburgh, PA, 1995, Gaussian 94, Revision D.4.

(19) Boys, S. F.; Bernardi, F. *Mol. Phys.* **1970**, *19*, 553.

(20) Hobza, P.; Burcl, R.; Špirko, V.; Dopfer, O.; Müller-Dethlefs, K.; Schlag, E. W. *J. Chem. Phys.* **1990**, *101*, 990.

(21) Gerhards, M.; Kleinermanns, K. *J. Chem. Phys.* **1995**, *103*, 7392.

(22) Janzen, C.; Spangenberg, D.; Roth, W.; Kleinermanns, K. *J. Chem. Phys.* **1999**, *110*, 9898.

(23) (a) Tanabe, S.; Ebata, T.; Fujii, M.; Mikami, N. *Chem. Phys. Lett.* **1993**, *215*, 347. (b) Watanabe, T.; Ebata, T.; Tanabe, S.; Mikami, N. *J. Chem. Phys.* **1996**, *105*, 408.

(24) Gerhards, M.; Schiwek, M.; Unterberg, C.; Kleinermanns, K. *Chem. Phys. Lett.* **1998**, *297*, 515.

(25) Courty, A.; Mons, M.; Dimicoli, I.; Piuzzi, F.; Brenner, V.; Millié, P. *J. Phys. Chem. A* **1998**, *102*, 4890.

(26) Piest, A.; v. Helden, G.; Meijer, G. *J. Chem. Phys.* **1999**, *110*, 2010.